Sample-dependent optical dephasing in bulk crystalline samples of Y_2O_3:Eu^{3+}

G. P. Flinn, K. W. Jang, Joseph Ganem,* M. L. Jones, and R. S. Meltzer
Department of Physics and Astronomy, University of Georgia, Athens, Georgia 30602-2451

R. M. Macfarlane
IBM Research Laboratories, Almaden, San Jose, California 95193
(Received 29 October 1993)

Two-pulse photon-echo measurements were made on the $^7F_0 \leftrightarrow {}^5D_0$ optical transition in a number of crystalline samples of Y_2O_3:Eu^{3+} prepared by three different crystal-growth techniques. For crystals prepared by a laser-heated pedestal growth or arc-imaging furnace process, we report the observation of an additional sample-dependent contribution to the optical dephasing in comparison with a crystal grown by flame fusion. The dephasing rate $1/T_m$ at 1.4 K is up to two orders of magnitude faster than that previously reported for the flame-fusion-grown crystal, and is uncorrelated with concentration. Measurements up to 14 K show that $1/T_m$ increases linearly with temperature, in contrast to the expected T^7 behavior due to a two-phonon Raman process. The linear temperature dependence is similar to that seen in glasses and disordered crystalline systems, suggesting the presence of disorder in the samples with more rapid dephasing. The crystals were examined by x-ray diffraction, excitation spectroscopy, and near-field optical microscopy to provide information on the nature of the disorder. The effect of annealing on the crystal dynamics is also investigated.

INTRODUCTION

Progress in optical technology has depended on the ability to manufacture materials with good and consistent optical properties. In particular, the introduction of defects, strains and other disorder during the preparation of crystalline materials can adversely affect many of these optical properties, and thus an understanding of the general nature of disorder and how this comes about during the growth process is of critical significance.

The dynamical behavior of impurity ions can serve as a sensitive probe of the disorder because the optical dephasing in ordered crystalline environments is generally quite distinct from that of amorphous or disordered systems. In disordered systems the dephasing is controlled by the interaction of the impurity ions with low-frequency modes of the host lattice, also known as two-level systems, or TLS.[1] In dilute ordered crystalline materials at low temperatures, the dephasing is largely dominated by interactions between the electronic or nuclear moment of the impurity ions and those of the host constituents.[2] As a result, the magnitude of the homogeneous optical linewidth (Γ_H) in disordered systems is many orders of magnitude greater than in ordered crystalline materials, and the temperature dependence of Γ_H is also quite different.[1] In the present paper, we study the optical dephasing of a number of crystalline samples of Y_2O_3:Eu^{3+} prepared by three different crystal-growth techniques, and present evidence for dynamical properties of some of these samples which are characteristic of disordered systems.

The dynamical environment of impurity ions doped into host materials can be probed by transient spectroscopic techniques such as the two-pulse photon echo.[1-3] Measurement of the echo intensity as a function of the preparation pulse separation (i.e., the echo decay) reveals the dephasing time T_2 (or more generally, the phase memory time T_m), which is directly related to the homogeneous linewidth of the transition ($\Gamma_H = 1/\pi T_m$). Furthermore, the form of the echo decay and its temperature behavior can also yield information relating to the mechanisms responsible for the dephasing process.[1,2]

The $^7F_0 \leftrightarrow {}^5D_0$ transition for Eu^{3+} doped into Y_2O_3 has been previously reported to have an extremely long dephasing time at low temperature.[4-6] This arises because of the nearly nonmagnetic character of the host, the very small magnetic moment ($\leq$kHz/G) of the ground and excited states of the Eu^{3+} ion (nuclear in origin), the energetic isolation of these two levels, and ultimately the metastability of the $^5D_0$ excited state (lifetime $\sim$0.9 ms). Measurements made using two-pulse photon echoes reveal a homogeneous linewidth of only 760 Hz in the wings of the inhomogeneous line.[4] Toward the center of the line, excitation-induced optical-frequency shifts lead to a more rapid dephasing of the transition,[6] and Γ_H was measured to be 2.5 kHz. The temperature dependence of Γ_H between 12 and 35 K is consistent with a two-phonon Raman process.[7] The long coherence times presented by the Eu^{3+} ions in this environment thus provide a very sensitive probe of the dynamics of the crystalline system.

The experiments described here were made on Y_2O_3:Eu^{3+} samples grown by three different methods; (i) six crystalline fibers (diameter $\sim$0.4 mm, concentration in the range 0.004–0.55 at. % Eu^{3+}) grown by laser-heated pedestal growth (LHPG)[8] and labeled as fibers $F1$ to $F6$; (ii) a $\sim$0.1 at. % crystal grown in an arc-imaging furnace,[9] referred to as the arc crystal; and (iii) a sample grown by the Verneuil process, or flame fusion,[10] referred to as the flame-fusion crystal, and which has been studied by a number of previous authors.[4-7] The fluorescence

lifetime of the $^5D_0$ excited state in each of the samples is the same as that observed in the flame-fusion crystal, and all of the samples show a similar inhomogeneous absorption linewidth characterized only by a concentration-dependent broadening (5→25 GHz) as would normally be expected for rare-earth-doped insulators. However, measurements made at 1.4 K of the phase memory time (T_m) of the $^7F_0 \leftrightarrow {}^5D_0$ transition in the six fibers and the arc crystal reveal that it is up to two orders of magnitude shorter than that previously reported in the flame-fusion crystal, and the dephasing is found to be uncorrelated with the europium concentration. Furthermore, the temperature dependence of the dephasing rate ($1/T_m$, and thus a measure of Γ_H) is also distinct from that observed in the flame-fusion sample; the temperature dependence is nearly linear at low temperatures (1–12 K), as opposed to the T^7 Raman behavior previously reported.[7] A nearly linear temperature dependence in the dephasing rate is generally characteristic of disordered systems, and has been, for example, observed in Eu^{3+}-doped silicate glass.[11] Some of the samples were examined by x-ray diffraction and near-field optical microscopy, and the effect of annealing on the dephasing was also investigated.

EXPERIMENT

The fibers were grown by a laser-heated-pedestal-growth technique,[8] one of a number of methods available for the rapid preparation of crystalline materials. A sintered preparation material was melted at its upper end at the focus of a CO_2 laser. A seed crystal was then dipped into the melt, and a fiber of the material was drawn at a rate of about 1 mm/min. The resulting fibers were ~400 μm in diameter and some millimeters in length. The ends of each of the fibers were then polished, and a focused laser beam was observed to pass relatively unheeded through its length. The six fibers $F1$–$F6$, and the flame-fusion and arc crystals were all mounted on the same sample holder, and placed in a helium-immersion cryostat equipped with optical windows. For experiments at 1.4 K, the sample chamber could be filled with liquid helium from the reservoir, and the helium pumped below the λ point. For experiments above 1.8 K, a small heating element allowed a trickle of helium liquid from the reservoir to be warmed before it passed to the samples. The temperature could be varied from 2 to 14 K, with a stability of ±0.2 K, and an accuracy ranging from ±0.1 at 4.5 K, to ±1 at 14 K.

Optical excitation of the transition was accomplished using a Coherent 599-21 single-frequency dye laser (jitter ~2 MHz), operating with Rhodamine R6G at the 5808-Å Eu^{3+} $^7F_0 \leftrightarrow {}^5D_0$ absorption. The laser beam was optically gated using two acousto-optic modulators operating in tandem; two were used to ensure sufficient rejection of the laser radiation during the off period (rejection 10^{-5} or 10^{-6}). Optical pulse durations for the experiments were typically 600 ns ("$\pi/2$" pulse) and 850 ns ("π" pulse), and were directed into the cryostat windows through a 30-cm lens (spot size at the crystals was ~50 μm). Laser power (cw) at the cryostat window was ~10 mW. A good and reproducible launch into the fibers, without incurring any internal reflections, could be made by looking for a clear transmitted-beam spot on the detection side of the cryostat. A particular path could be identified by collimating the output light with a second lens, and observing the spot as the beam was translated across the entrance face of the fiber. Passage of the laser beam off axis through the fiber could clearly be seen as distortion of the output spot. The echoes were detected using a photomultiplier (EMI 9558) and transient digitizer. A double Pockel's cell arrangement was used to temporally protect the photomultiplier from the transmitted preparation pulses (rejection 10^5) by gating the cells after the second preparation pulse. The photon echo at each pulse separation was averaged for 100–2000 pulse pairs (repetition rate 10 Hz), and the data recorded on a computer.

Care was taken to avoid problems associated with holeburning of the Eu^{3+} transition, since the lifetime of the holes at liquid-helium temperatures may amount to several days.[7] During alignment of the laser beam through the fiber, and the positioning of the detection optics, the pulse repetition rate was increased to ~100 kHz in order to view the transmitted beam. To avoid holeburning, this step in the experiment was made with the laser detuned from the transition, and it was only returned to line center when the repetition rate had been reduced to 10 Hz. Furthermore, all the echo decay measurements and optics alignment tasks were made with the laser scanning over about a 0.6-GHz range at approximately 1 Hz.

RESULTS

Photon-echo decay curves for some of the fibers are shown in Figs. 1(a) and 1(b). All measurements were made at 1.4 K at the center of the absorption line. Instantaneous diffusion effects were observed in the flame-fusion sample, which appears as a variation of Γ_H over the inhomogeneous line as has been previously reported.[4–6] No such instantaneous diffusion was apparent in the dephasing of the fibers, or in that of the arc crystal. Similarly, no change in the dephasing time was observed either for changes in the pulse area, or for changes in the pulse intensity by a factor of 2 (limited by the weakness of the echo signal, especially in the fibers). As can be seen in Fig. 1(a), fibers $F1$ and $F3$ exhibit an obvious nonexponential character to the dephasing, and this feature is also observed in fibers $F2$ and $F6$. In the instance of a nonexponential echo decay, the dephasing is best described in terms of the phase memory time T_m, and a fit of the form

$$I = I_0 \exp\left\{\frac{-4\tau}{T_m}\right\}^X \tag{1}$$

was made to the data.[12,13] I is the echo intensity measured at each pulse separation τ, and X is the nonexponential fitting parameter; if X is set equal to 1, then $T_m = T_2$ and the fit is exponential. In Fig. 1(a) we also show measurements of fiber $F1$ both for a 6-mm-length

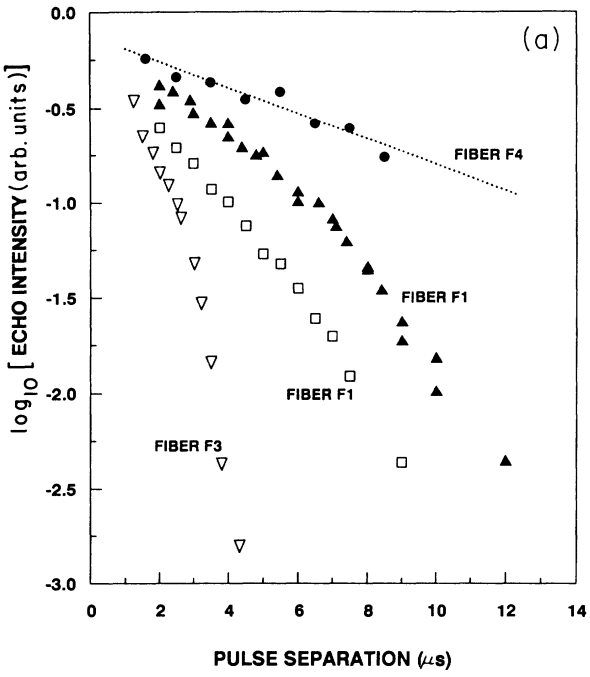

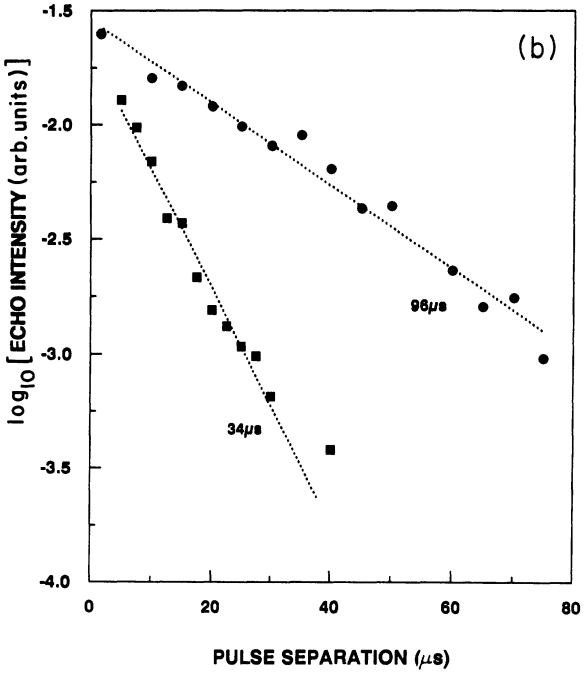

FIG. 1. (a) Echo decay curves for fibers $F1$ and $F3$ at 1.4 K. The echo decay can be followed for at least two orders of magnitude, thus clearly showing the difference in the dephasing rates of the different fibers. Fibers $F1$ and $F3$ exhibit a clear nonexponential echo decay, whilst fiber $F4$, shown here only in part, characteristically exhibits an exponential decay. The upper and lower echo decays for fiber $F1$ are for a 6-mm length of fiber, and for 1-mm piece cut therefrom, respectively. (b) Two different echo decay curves for fiber $F4$, both measured at the same temperature (1.4 K). The two decays correspond to two different optical paths through the fiber.

sample, and for a 1-mm length cut from the original 6 mm.

Table I summarizes various spectroscopic data obtained for all samples. Except where indicated, all data are for a temperature of 1.4 K. The Eu^{3+} concentration in each fiber was determined by integrating the absorption coefficient over the inhomogeneous line and comparing these with that measured for the flame-fusion crystal, where the Eu^{3+} concentration has been determined by electron-beam microprobe analysis as 0.3 at.%. It should be noted that the fluorescence lifetime of all the fibers, and that of the arc crystal, are all nearly identical to that of the flame-fusion crystal. In addition, the inhomogeneous linewidths of the Eu^{3+} $^7F_0 \leftrightarrow {}^5D_0$ transition in fibers $F1$ and $F5$ are also comparable to that of the flame-fusion crystal, and in general the inhomogeneous linewidths vary monotonically with concentration as would normally be expected.

It is seen in Table I that all the samples exhibit shorter values of T_m than the flame-fusion crystal, and in fibers $F2$, $F3$, and $F5$, and in the arc crystal, this is by more than an order of magnitude. We refer to this dephasing as being anomalous with respect to that of the flame-fusion crystal. Fibers $F1$, $F2$, and $F3$ exhibit not only a very rapid dephasing, but also show a strong nonexponential character to the echo decay ($X > 1$). The spread in values determined for X (median of ~ 2) partially reflects the short time scale over which an echo decay could be measured. Where X is observed to be greater than 1, then the dynamical processes are responsible for a spectral diffusion which occurs over the time scale of the echo measurements. Fiber $F6$ also shows a nonexponential form to the dephasing, where X is measured consistently to be ~ 1.5, but is characterized by a much longer value for T_m. In fact, the phase memory time at 1.4 K (80 μs) compares favorably with the value of 130 μs measured by us in the flame-fusion crystal at line center. Fiber $F4$ exhibits another general aspect of the observed dephasing, as shown in Fig. 1(b); it is possible to observe different values for T_m by arranging for different beam paths through the fiber. For one beam path, $T_m = 34$ μs, whereas subsequent measurements over a different beam path gave $T_m = 115$ μs. Similarly, some degree of spatial inhomogeneity in the dephasing was observed in most of the fibers. Finally, the dephasing observed in the arc crystal is also rapid, but is characterized by an exponential echo decay.

Figure 2(a) shows the temperature dependence of the optical dephasing rate ($1/T_m$) for three of the fibers ($F1$, $F2$, and $F3$), and the flame-fusion and arc crystals. While the flame-fusion sample shows a nearly temperature-independent rate until the onset of the two-phonon Raman process,[7] each of the other samples shows an additional contribution to the overall dephasing rate which has a nearly linear temperature dependence. For the fibers $F1$ and $F2$, where most of the measurements were made because of their strong echo signals, we found that the dephasing rate is indeed linear in temperature. Figure 2(b) depicts the same measurements made on fibers $F4$ and $F6$, illustrated on an expanded scale. For one beam path through fiber $F4$, where $T_m = 115$ μs (at 5 K),

TABLE I. Values for the lifetime of the $^5D_0$ excited state, the inhomogeneous absorption linewidth, the phase memory time T_m and associated nonexponential fitting parameter X, and the measured concentration of Eu^{3+} for each of the fibers, and for the arc and flame-fusion samples. All experiments made to determine these parameters were undertaken at 1.4 K.

Sample	Eu content (at. %)	T_m (μs)	$^5D_0$ lifetime (μs)	Inhomogeneous absorption linewidth (GHz)	Nonexponential parameter X
Fiber $F6$	0.55	80	950±30	23.4±2.1	1.5
Fiber $F1$	0.3	$17\frac{1}{2}$	900±20	11.3±0.3	1.5–2.5
Fiber $F5$	0.13	$\sim 7\frac{1}{2}$	940±30	6.4±0.2	· · ·
Fiber $F2$	0.1	12.2	940±20	7.1±0.5	1.5–2.5
Fiber $F3$	0.05	8.3	950±20	5.4±0.3	1.5–2.5
Fiber $F4$	0.004	34,115[a]	880±20	5.5±0.8	1
flame fusion	0.3	130	915±10	7.1±0.5	1
arc	~0.1	12	≈900	≈90±20	1

[a]Value measured at 5 K; see discussion in text.

the value lies very close to that measured in the flame-fusion sample at the same temperature. The dephasing rates for fibers $F4$ and $F6$ at higher temperatures converge with the T^7 Raman behavior of the flame-fusion crystal. Even though the anomalous contribution to the dephasing is small in these two fibers, a nearly linear temperature dependence appears.

DISCUSSION

We first consider the dephasing mechanisms normally expected in Y_2O_3:Eu^{3+}. At the low concentrations present in these samples, we can safely ignore any contribution made by Eu^{3+}-Eu^{3+} interactions. Thus, at low temperatures, the magnetic interactions of the Eu^{3+} ions with the host ^{89}Y nuclear moments are expected to play an important role in the dephasing. This is the case in the flame-fusion sample, and it is partly because of the very small value of the ^{89}Y nuclear moment (0.21 kHz/G) that such long dephasing times are observed. Estimates for this contribution of ≤ 100 Hz are consistent with the observed value of T_m.[4] No temperature dependence from this process is predicted, and indeed the flame-fusion sample shows a temperature-independent dephasing below 8 K.

Phonon-induced contributions to the dephasing become important only above 8 K since both the $^7F_0$ ground state and $^5D_0$ optically excited states are singlets and are well isolated energetically from their nearest electronic states. Resonant phonon interactions via the direct process are absent for $^5D_0$ (nearest electronic state ≈ 1700 cm^{-1}), and should be negligible for $^7F_0$ below 10 K since the direct phonon contribution is[14]

$$T_2^{-1} = T_1^{-1} \exp\{-\Delta/kT\} , \quad (2)$$

where $T_1 \approx 10^{-12}$ s is the estimated spontaneous relaxation time of the lowest excited state of $^7F_1$ at an energy of $\Delta = 200$ cm^{-1} above the ground state.[15] We estimate a contribution to the dephasing for direct processes of less than 1 Hz at 10 K. In fact, the two-phonon Raman process dominates here, and its onset at about 8 K can be seen in Figs. 2(a) and 2(b) as a T^7 temperature dependence to the dephasing rate for the flame-fusion sample.[7]

Defect centers possessing an electronic magnetic moment can provide an additional source of optical dephasing. Mutual spin flips among these centers could produce fluctuating magnetic fields at the europium sites. The required concentration of $g=2$ centers which could produce sufficiently high fields at the Eu^{3+}-ion sites is estimated to be ~0.1%. Such a large concentration of electron spin defects is highly unlikely. In addition, the contributions of mutual spin flips among these centers would be strongly magnetic-field dependent, as the electronic spins would be partially frozen in their ground states at large fields at these low temperatures. However, the anomalous dephasing shows no magnetic-field dependence for fields up to 5 kG, the maximum field examined.

Instantaneous diffusion has been observed in the flame-fusion crystal by Huang and co-workers.[6] This refers to the instantaneous frequency shift of the transition induced by the simultaneous excitation of nearby ions (thus changing the local field), and is observed as a variation in the dephasing time over the inhomogeneous line. The effect is simply related to the number of ions excited by the second pulse, and should thus scale with the Eu concentration (and hence position within the inhomogeneous line), the frequency bandwidth, and the laser power. It should also be relatively independent of temperature. Although we have observed a frequency-dependent dephasing in the flame-fusion crystal, this is not the case for any of the other samples, and we also observe no power dependence. In general, the more rapid dephasing in these samples makes them insensitive to these effects.

The results clearly indicate that an additional component to the dephasing is present in the arc and fiber samples, augmenting the dynamical environment of the

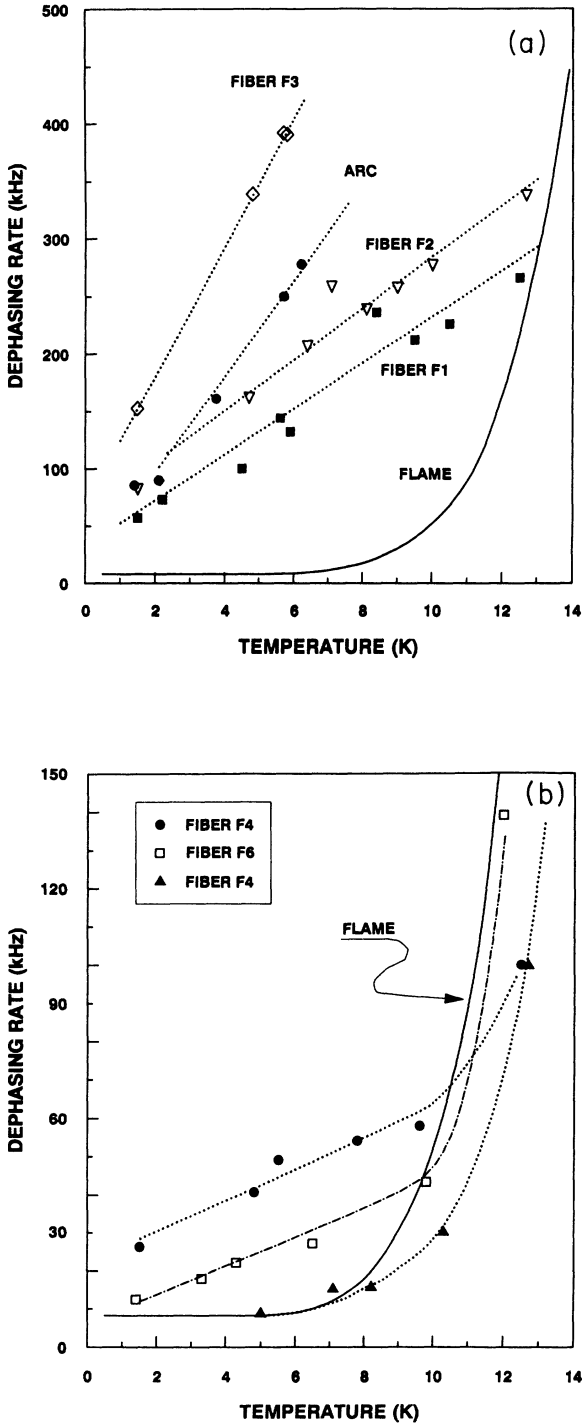

FIG. 2. (a) Temperature dependence of the dephasing rate $(1/T_m)$ for fibers $F1$, $F2$, and $F3$, and for the arc and flame-fusion samples. Fibers $F1$ and $F2$ clearly follow a $\sim T^{1.0}$ dependence; the dotted lines represent linear fits to each data set. The solid curve shown for the flame-fusion crystal represents the T^7 Raman behavior observed for this crystal (Ref. 8); dephasing rates measured by us in this crystal as a function of temperature all lie close to this line (within the measured temperature uncertainty). (b) Same data for fibers $F4$ and $F6$, again in comparison with the flame-fusion crystal, shown on an expanded scale. Note the two sets of data for fiber $F4$. The dotted and broken lines are a guide only.

dopant ions. It is well documented that glasses and disordered crystalline systems exhibit a more rapid optical dephasing, and that this dephasing depends approximately linearly on temperature (1–20 K).[1] The dynamics of these hosts is ascribed to two-level systems (TLS).[1] For example, measurements of persistent spectral holeburning of molecules in organic glasses shows $\sim T^{1.3}$ dependence of the linewidth at low temperatures (0.3–20 K).[1] Similar results are observed for rare-earth ions in inorganic glasses; Eu^{3+} in silicate glass shows $\Gamma_H \sim T^{1.0}$ up to 4 K;[11] and for Pr^{3+} ions, also in silicate glass, $\Gamma_H \sim T^{1.0}$ up to 20 K.[16] Disordered crystalline systems also show a similar temperature behavior. For example, Pr^{3+} in yttria-stabilized zirconia, which has the fluorite structure with a random distribution of oxygen vacancies, also shows a large homogeneous linewidth which depends on temperature as $T^{1.2}$.[17] In a mixed solution crystal of $BaFCl_{0.5}Br_{0.5}$, the linewidth of persistent spectral holes of Sm^{2+} ions obtained by photoionization follow a $T^{1.0}$ dependence.[18]

Briefly, the TLS result in configurational changes of the local structure of the host lattice. These occur over a broad range of time scales, and there exists a wide spectrum of excitation frequencies for the TLS with a nearly constant density of states.[1] The data presented here for these crystalline samples of Y_2O_3 shows behavior quite similar to that of disordered materials. Although it is apparent that the magnitude of the dephasing lies somewhat midway between that of good crystalline material and that of disordered systems, the nearly linear temperature dependence of the dephasing implies a broad distribution of excitation frequencies for the modes responsible for the dynamics. In addition, the nonexponential nature of the echo decay in most of the samples indicates the presence of spectral diffusion, a characteristic in glasses whose dynamics are controlled by TLS.[1] Spectral diffusion has in fact been directly observed in one of the fiber samples using ultranarrow holeburning techniques. In experiments performed on fiber $F5$, the hole width was observed to broaden sublinearly with time over a period spanning milliseconds to seconds; this broadening results from the spectral diffusion process on the linewidth of the transition.[19]

The question then arises as to what sort of modes are responsible for the dynamics of Y_2O_3:Eu^{3+}. In glasses and other disordered systems, there is, in addition to the much larger homogeneous linewidths, a large inhomogeneous linewidth associated with the wide range of local environments. Furthermore, the range of local sites leads to a nonexponential radiative decay due to the wide range of resulting lifetimes. We considered the possibility of small, highly distorted regions in the samples where TLS might result in glasslike dynamics. Although the majority of the Eu^{3+} ions would be at normal crystal sites, the TLS could couple weakly (due to larger distances) to these sites, thereby producing the anomalous dephasing, but still allowing the exponential radiative decay of the $^5D_0$ excited state and the absorption line shape and width characteristic of a crystal. However, a small fraction of the Eu^{3+} ions should therefore have sufficient proximity to the distorted sites, and their existence would lead to a

broad absorption pedestal around the normal site absorption. We obtained an excitation spectrum of the Eu^{3+} ions in a number of the samples up to 100 cm^{-1} below the main line by monitoring fluorescence in the region of the $^5D_0 \rightarrow {}^7F_2$ transition. While the arc crystal possesses two additional absorption lines about 54 and 104 cm^{-1} from the main transition,[20] we could not in general detect any broad background to the crystalline absorption in any of the samples. While we cannot exclude these distorted-ion sites, we can estimate an upper limit; for an absorption band about 30 cm^{-1} wide (120 times broader than the majority-site absorption) and a detection sensitivity of 10^{-6} that of the main site, we may conclude that no more than 10^{-4} of the Eu^{3+} ions exist within these regions.

To further address the question of the type of disorder present in these samples, x-ray-scattering measurements were made on some of the samples. The diffraction patterns clearly indicate the presence of well ordered Y_2O_3. In addition, several of the fibers were annealed (fibers $F3$, $F4$, and $F5$), and so was a portion of the arc crystal; if there are regions of disorder within the samples, it might be possible to modify the dynamics by allowing these regions to reform as crystalline areas. The annealing process involved maintaining the crystals at 2000 °C for half an hour, and upon cooling the optical dephasing of these samples was then remeasured. Whilst fiber $F3$ did show a reduction in the nonexponential behavior of the echo decay (albeit without a significant change in T_m), the dephasing measured in the arc crystal remained as before. Fibers $F4$ and $F5$ also showed no change in their dephasing times. Indeed, it should be noted that within the context of the observed spatial inhomogeneity of the dephasing, little change was actually observed in any of the samples. Thus we cannot conclude that the annealing made any significant difference to the dynamics.

Some fibers and the arc crystal were examined by near-field optical microscopy. A laser confocal microscope is used to examine different planes within each sample, where the depth of field and the optical resolution make the microscope capable of resolving detail only 1 μm in size. The structure of each of the samples examined was observed to contain different features that all appear to be artifacts of the growth process. In particular, it appears that the fiber growth was both nonreproducible and nonsymmetrical, and results in an internal structure of the sample. Through the microscope, this internal structure was observed to comprise microbubbles, distinct variations in the refractive index, and areas of a polycrystalline nature. Each of these defects were observed to be dominant in different samples, and each were distributed inhomogeneously over the fiber cross section. For example, the arc crystal was found to principally contain microbubbles, whose dimensions vary from the minimum resolution up to about 10 μm. These microbubbles were seen to be randomly distributed throughout the crystal, with the average density increasing radially from the center of the growth axis of the crystal. The maximum bubble density is estimated to be $\sim 10^6$ cm^{-3}. In general, both the laser-heated-pedestal and the arc-imaging growth processes are characterized by their unstable growth environments. For example, in LHPG, drift in the CO_2 laser power leads to temperature and volume fluctuations of the melt. Similarly in the arc-imaging process, the incorporation of defects during the growth is known to be critically dependent on both the temperature gradient and the growth rate.[9] At sufficiently slow arc-imaging growth rates, the growth becomes unstable and voids (or microbubbles) are introduced into the crystal.

Although the macroscopic defects in these samples may account, at least qualitatively, for the variety in the dynamics observed, evidence exists in the data to infer the role of microscopic defects in the dephasing. The fact that the nonexponential parameter X is generally greater than 1 indicates that there are few Eu^{3+} ions sufficiently decoupled from the increased dynamical activity to exhibit a low dephasing rate. Thus we may suppose that the defect structure responsible for the anomalous dephasing must be more homogeneous than the macroscopic defects observed, and that the range of coupling strengths of the impurity ions to the dynamics is then not especially broad. Oxygen nonstoichiometry is a probable point defect in this type of material. This is most likely to be in the form of vacancies, inducing a static disorder in the first two coordination shells of the cation, and leading to a charge redistribution that makes the Y-O bond more covalent.[21] It should be noted that this type of defect is not easily produced in yttria crystals (except by heating in a reducing environment), although the measurement techniques utilized in this investigation do appear to be sensitive to a very low degree of disorder.

SUMMARY

We have measured the optical dephasing of the $^7F_0 \leftrightarrow {}^5D_0$ transition in a number of crystals of Y_2O_3:Eu^{3+}, where production of the samples involved three different growth processes. The crystals produced by laser-heated pedestal growth and an arc-imaging process show a characteristically different dynamical behavior from the crystal grown by flame fusion. Instead of a slow dephasing rate, and a temperature dependence associated with a two-phonon Raman process, the LHPG and arc-imaging samples show a behavior akin to that observed in disordered systems; the dephasing rate is high and shows a nearly linear temperature dependence. This behavior is attributed to disorder present within the samples, where local configurational changes are then responsible for weak fluctuating fields at the Eu^{3+} sites, causing additional dephasing. In addition to the dephasing measurements, the sample properties were probed using x-ray diffraction, annealing, near-field optical microscopy, and excitation spectroscopy below the main absorption line. Despite the observation of macroscopic defects in the anomalous samples, disorder related to microscopic defects is a likely cause for the additional dephasing.

It should be noted that whilst the overall spectroscopic properties of a crystal (such as the radiative lifetime and the inhomogeneous absorption) may be similar in a range of samples prepared in different ways, the dynamical

behavior may be quite different. Time-domain spectroscopy thus provides a highly sensitive technique for materials characterization, and the intended application of a crystal may then dictate the requisite growth process to ensure adequate crystalline behavior. The role of physical disorder in the dephasing of optically excited ions forms an important topic as spectroscopic techniques become increasingly more sensitive, and materials such as Y_2O_3:Eu^{3+} then provide a sensitive environment in which to study this role.

ACKNOWLEDGMENTS

The authors wish to thank Lizhu Li for growing the fiber crystals, and Charles Greskovich of GE Corp. R&D for annealing some of the samples. Mark Farmer and Andrew Maselli of the Center for Ultra-Structural Research at UGA are acknowledged for their assistance with the near-field microscopy work. This work was supported by the National Science Foundation Grant No. DMR-9015468.

---

*Present address: Laser Physics Branch, Naval Research Laboratory, Washington, D.C. 20375.

[1]See, for example, R. M. Macfarlane and R. M. Shelby, in *Optical Linewidths in Glasses,* edited by M. J. Weber [J. Lumin. **36**, 179 (1987)]; D. L. Huber, in *Dynamical Processes in Disordered Systems,* edited by W. M. Yen (Trans Tech, Aedermannsdorf, Switzerland, 1989).

[2]R. M. Macfarlane and R. M. Shelby, in *Spectroscopy of Solids Containing Rare Earth Ions,* edited by A. A. Kaplyanskii and R. M. Macfarlane (North-Holland, Amsterdam, 1987).

[3]L. Allen and J. H. Eberley, *Optical Resonance in Two-Level Atoms* (Wiley, New York, 1975).

[4]R. M. Macfarlane and R. M. Shelby, Opt. Commun. **39**, 169 (1981).

[5]L. Root and J. L. Skinner, Phys. Rev. B **32**, 4111 (1985).

[6]Jin Huang, J. M. Zhang, A. Lezama, and T. W. Mossberg, Phys. Rev. Lett. **63**, 78 (1989); Jin Huang, J. M. Zhang, and T. W. Mossberg, Opt. Commun. **75**, 29 (1990).

[7]W. R. Babbitt, A. Lezama, and T. W. Mossberg, Phys. Rev. B **39**, 1987 (1989).

[8]R. S. Fiegelson, J. Cryst. Growth **79**, 669 (1986).

[9]H. Tsuiki, K. Kitazawa, T. Masamoto, K. Shiroki, and K. Fueki, J. Cryst. Growth **49**, 71 (980).

[10]R. A. Lefever and G. W. Clark, Rev. Sci. Instrum. **33**, 769 (1962); R. A. Lefever, *ibid.* **33**, 1470 (1962).

[11]Th. Schmidt, J. Baak, D. A. van de Straat, H. B. Brom, and S. Völker (unpublished).

[12]W. B. Mims, Phys. Rev. **133**, A835 (1964).

[13]Joseph Ganem, Y. P. Wang, D. Boye, R. S. Meltzer, and W. M. Yen, Phys. Rev. Lett. **66**, 695 (1991); R. S. Meltzer, Joseph Ganem, Y. P. Wang, D. Boye, W. M. Yen, D. P. Landau, R. Wannemacher, and R. M. Macfarlane, J. Lumin. **53**, 1 (1992).

[14]D. E. McCumber and M. D. Sturge, J. Appl. Phys. **34**, 1682 (1963).

[15]U. Köbler, Z. Phys. **247**, 289 (1971).

[16]P. M. Selzer, D. L. Huber, D. S. Hamilton, W. M. Yen, and M. J. Weber, Phys. Rev. Lett. **36**, 813 (1976); R. M. Macfarlane and R. M. Shelby, Opt. Commun. **45**, 46 (1983).

[17]K. Tanaka, T. Okuno, H. Yugami, M. Ishigame, and T. Suemoto, Opt. Commun. **86**, 45 (1991).

[18]K. Holliday, C. Wei, M. Croci, and U. P. Wild, J. Lumin. **53**, 227 (1992).

[19]M. J. Sellars, R. S. Meltzer, P. T. H. Fisk, and N. B. Manson (unpublished).

[20]Taking the main-line absorption as unity, the maximum absorption strengths of these subsidiary lines are approximately 10^{-2} and 10^{-4}, respectively.

[21]J.-P. Durand, F. Jollet, N. Thrornnat, M. Gautier, P. Maire, and C. le Gressus, J. Am. Ceram. Soc. **73**, 2467 (1990).